Nitrogen-boron Co-doping of Carbon-based ORR Catalysts

Undergraduate Thesis

Presented in Partial Fulfillment of the Requirements for Graduation with Research Distinction in the College of Engineering

The Ohio State University

William G. Lowrie Department of Chemical and Biomolecular Engineering

Autumn, 2019

Author

Corey Sceranka

Undergraduate Thesis Committee

Umit Ozkan, Advisor

Jeffrey Chalmers

Abstract

Diminishing fossil fuel resources and increasing concerns regarding climate change due to greenhouse gas (GHG) emissions have sparked research into clean energy alternatives. In the U.S., the transportation and electricity sectors heavily reliant on fossil fuels accounted for 56% of carbon dioxide emissions in 2016 [1]. Additionally, more than 90% of the fuels consumed in land, sea, and air travel are petroleum-based like gasoline and diesel, making transportation a target area for improvement [1]. A technology capable of replacing internal combustion engines within vehicular systems are hydrogen fuel cells (HFCs) which generate electricity through water-producing electrochemical reactions. One hurdle preventing large-scale commercialization of HFCs is the high loading of platinum (Pt) catalysts used to facilitate reactions in the cell, where Pt alone makes up 40% of total material cost [2]. A promising class of alternative catalysts include carbon-based catalysts capable of facilitating the cathodic oxygen reduction reaction (ORR). Doping these materials with heteroatoms can increase their ORR activity, and past studies have shown that both nitrogen and boron are good dopants to enhance ORR activities [3]. This research project investigates optimization of mono- and co-doping carbon catalysts with boron and nitrogen heteroatoms with the intent of improving ORR activity.

Acknowledgments

I would like to thank Dr. Umit Ozkan for allowing me to join the Heterogeneous Catalysis Research Group as an undergraduate student and Vance Gustin for being an invaluable mentor and amazing friend throughout my time with the group. Additional thanks go out to the other graduate and undergraduate students I had the pleasure of working with who've supported me along the way and the William G. Lowrie Department of Chemical and Biomolecular Engineering for providing ample opportunity for academic success within and outside the classroom.

Vita

May 2015……..……Kirtland High School

December 2019……..…B.S. Chemical Engineering, The Ohio State University

Fields of Study

Major Field: Chemical and Biomolecular Engineering

Table of Contents

List of Tables

List of Figures

Introduction

Background

Global reliance on fossil fuels for energy and transportation are leading contributors to the GHG emission problem. As society develops better awareness and understanding of climate change, the need for feasible clean energy alternatives is becoming more apparent. HFC technology is available for use today, but still faces commercialization hurdles such as scalability issues and high costs.

HFCs utilize electrochemical reactions to convert oxygen (O_2) and hydrogen (H_2) to water, thus generating clean electricity from renewable resources. The multi-electron cathodic reaction is slower than the anodic reaction because of reaction kinetics.

$$\text{Anode Reaction:} \quad 2H_2 \rightarrow 4H^+ + 4e^-$$

$$\text{Cathode Reactions:} \quad 2H^+ + 2e^- + O_2 \rightarrow H_2O_2$$

$$H_2O_2 + 2H^+ + 2e^- \rightarrow 2H_2O$$

$$4H^+ + 4e^- + O_2 \rightarrow 2H_2O$$

$$\text{Overall Reaction:} \quad 2H_2 + O_2 \rightarrow 2H_2O$$

Both are facilitated through state-of-the-art precious metal catalysts, but the slower cathodic kinetics require a higher catalyst loading. The precious metals in these state-of-the-art high catalysts are usually Pt or palladium (Pd), and the high cathodic loading of either greatly increases the cost of the system [3]. Pt is an exceptional catalyst for the hydrogen oxidation reaction at the anode, but on the cathode O_2 reduction is slow, especially at HFC operating temperatures, thus requiring a high loading of Pt to increase the overall cathodic reaction rate [4, 5]. Developing an effective substitute for these materials could lower the price barrier to HFC technology commercialization. A problem that these high-performing precious metal catalysts face is chemical poisoning, but this can be overcome through use of carbon-based catalysts.

Heteroatom-doped carbon-based ORR catalysts have shown resistance to various poisons that greatly hinder Pt catalyst performance [6], [7]. Boron-doped carbon-based materials have demonstrated immunity to both methanol and CO poisoning, both of which bind to precious metal active sites and reduce catalytic performance [6]. Additionally, nitrogen-doped materials have demonstrated resistance to CO and cyanide, which poisons precious metal catalysts by leeching out their active sites [7]. No change in CO concentration was reported at high or low concentrations when the gas was passed over nitrogen-doped materials, suggesting material immunity to CO poisoning [7]. CO sources generally include contaminates in the hydrogen fuel source, so reducing the poisoning effects of CO to the ORR catalyst would be important to its commercialization. Under mass production, this allows hydrogen fuel to not be as rigorously

treated for potential poisons that would typically inhibit a Pt catalyst containing system, further reducing overall HFC costs and increasing simplicity.

The cathodic reactions aren't always one step and may lead to the intermediate production of hydrogen peroxide (H_2O_2). If H_2O_2 accumulates before being reduced to water, it will degrade the carbon catalyst and be detrimental to system performance, therefore developing catalysts with high selectivity for one-step full reduction of oxygen to prevent any accumulation of H_2O_2 is also crucial.

Research Significance

Both boron-doped and nitrogen-doped materials have experimentally shown ORR activity increases without being co-doped [9]–[11]. A study performed by Chen, Xin et al. [8] explores the complexities of doping specific graphyne sites with boron or nitrogen. Boron doping generates ORR active sites at the boron atom because of its partial positive charge resulting from electronegativity differences with carbon. Conversely, nitrogen doping active sites are the carbons around the incorporated nitrogen atom.

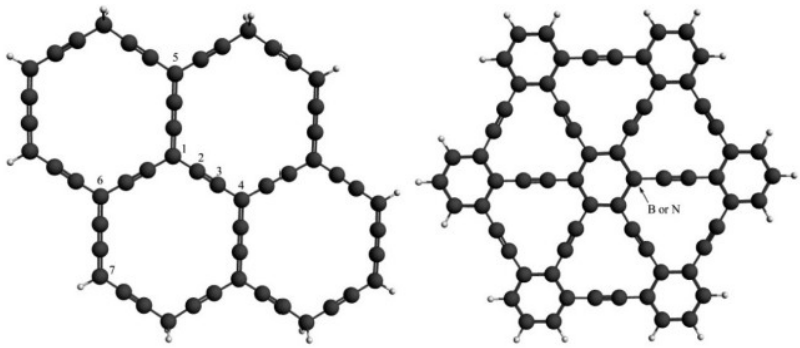

Figure 1: Configurations of (a) α- and (b) γ-graphyne w/ gray C and white H atoms [8]

Error! Reference source not found. shows the notation of carbon atoms in the two graphyne configurations studied. For mono-doped α-graphyne, the best boron doping stability was observed at site 1, denoted α-B_1G, while the best nitrogen doping stability was observed at site 2, denoted α-N_2G, and both boron and nitrogen were edge doped at site 7.

$$O_2 + H^+ + e^- \rightarrow *OOH \quad (1)$$

$$*OOH + H^+ + e^- \rightarrow *O{-}H_2O \quad (2)$$

$$*O{-}H_2O + H^+ + e^- \rightarrow *OH + H_2O \quad (3)$$

$$*OH + H^+ + e^- \rightarrow H_2O \quad (4)$$

$$\text{overall:} \quad O_2 + 4H^+ + 4e^- \rightarrow 2H_2O \quad (5)$$

Figure 2: Simulated ORR reaction mechanism [8]

Following the studied reaction mechanism depicted in **Error! Reference source not found.**, co-doped models showed more favorable ORR catalytic potentials than their mono-doped counterparts in all (α-B_1N_3G, α-B_1N_4G, α-$B_1(N_4)_3G$) but one (α-B_1N_2G) configuration. Additionally, both γ-BG and γ-NG were stable and showed favorable catalytic activity, but they followed a very different reaction mechanism than shown in **Error! Reference source not**

found. and still were outperformed by co-doped graphyne. To summarize this study, it is expected that co-doped catalysts will outperform their mono-doped counterparts and the same synergistic effects will be observed in graphene as demonstrated in graphyne.

Overview of Thesis

An analysis of HFC systems reveals that a large commercialization hurdle can be overcome by developing cost effective heteroatom-doped carbon-based catalysts as replacements for precious metal cathodic ORR catalysts, and previous research has shown that both boron and nitrogen are effective dopants for increasing ORR activity [8]. Nitrogen-doped carbon-based materials (CN_x), boron-doped carbon-based materials (CB_y), and nitrogen-boron co-doped carbon-based materials (CN_xB_y) will be synthesized through different methods. Once multiple doped samples have been synthesized, they will be tested following a standardized cyclic voltammetry (CV) procedure in a three-electrode half-cell system, and the gathered data will then be analyzed for ORR performance differences due to mono- and co-doping as well as differences due to variety in synthesis methods.

Methodology

Synthesis

To synthesize CN_xB_y, a precursor was made using wet impregnation (WI) of iron(II) acetate (FeAc), magnesium oxide (MgO), and boric acid (H_3BO_3). A molar ratio of 3:1 B:Fe was calculated and weights of 124.6 mg, 132.9 mg, and 2.000 g of FeAc, H_3BO_3, and MgO were used, respectively. These were combined in 100 mL of DI water, and the suspension was partially evaporated down to 50 mL before being placed in an oven at 110° C to dry overnight. The precursor was next ball milled at 200 rpm for 3 hours. 900 mg of the ball milled precursor was then weighed out for a chemical vapor deposition (CVD) treatment. The precursor was loaded into a quartz boat and placed into a quartz tube. The tube was then inserted into a furnace with the boat loaded in the center of the furnace, and inlet and outlet gas lines were attached to the tube. The acetonitrile (CH_3CN) bubbler was then purged with nitrogen gas before the flow was switched to the bypass line and purged. The furnace was then heated to 900° C at 10° $C*min^{-1}$. Once the furnace reached temperature, the gas flow was switched from the bypass to the bubbler, and the precursor was treated for 2 hours. After the allotted time, the gas flow was switched back through the bypass, the furnace was turned off, and the material was allowed to cool to room temperature overnight under a nitrogen atmosphere. Finally, the material was recovered from the CVD furnace and washed with 1 molar hydrochloric acid (HCl), vacuum

filtered with 2 filter pads, and washed with 1L of deionized (DI) water before being placed into an oven at 60° C to dry overnight. The finished catalyst was then recovered and stored for testing.

To synthesize CB_y-WI, a precursor was made by performing a WI of a 1:5 weight ratio mixture of graphene oxide (GO) and H_3BO_3. 300 mg of GO were mixed with 1500 mg of in a solution containing 50 mL of ethanol and 50 mL of water in a 70° C water bath. This was then covered with perforated foil and allowed to evaporate until 50 mL of the solution remained, then the rest was evaporated in an oven at 60° C overnight. Once fully dry, the precursor was recovered and put through an argon shock treatment. 1.000 g of the sample was weighed out for the shock and spread evenly across the length of a quartz boat. The loaded boat was then put into a quartz tube with inlet and outlet gas lines attached. The shock furnace was heated to 950° C at a rate of 15° $C*min^{-1}$ with argon flowing through the tube. Once the furnace reached temperature, the sample was centered into the furnace using a magnetic rod and shock treated under the argon atmosphere for one hour. After the hour was up, the furnace was turned off and the tube was removed from the furnace and allowed to cool under room temperature while under an argon atmosphere. Once the tube had reached room temperature, the CB_y-WI final sample was recovered and stored for testing.

To synthesize CB_y-TA, a catalyst-free thermal annealing (TA) method was referenced [12]. A 1:2 weight ratio GO to boron oxide (B_2O_3) was weighed out, 500 mg of B_2O_3 and 250 mg of GO.

The B_2O_3 was first spread evenly across the length of a quartz boat, then evenly and completely covered with the GO. The loaded boat was then inserted into a quartz tube and the boat was centered into the furnace. While under an argon atmosphere, the loaded tube was heated in the furnace to 1050° C at a rate of 15° C*min^{-1}. The sample was then treated for 4 hours at temperature, and after the allotted time the furnace was turned off so the tube could cool to room temperature in the furnace while still under argon. The recovered material was then washed in a 3 molar sodium hydroxide (NaOH) solution. 250 mL of 3M NaOH was used to wash the material overnight, and then the solution was vacuum filtered using 2 filter pads and rinsed with 1L of DI water. The filter pads were then placed in a beaker and transferred to an oven at 60° C to dry overnight. The final CB_y-TA sample was then recovered from the dried filter pads and stored for testing.

The CB_y-TA procedure was further modified for a different batch of catalyst [12]. One difference being that the weight ratio of B_2O_3 to GO was changed to 1:1. The starting materials were still layered and heated at the same temperature for the same duration. Additionally, the material was washed in 3M NaOH, but only for 2.5 hours instead of overnight.

To synthesize CN_x, a pyrolysis procedure was referenced [13] . A precursor was generated using an incipient wet impregnation (IWI) of FeAc and MgO, which was then dried in an oven at 110° C overnight and then ball milled at 200 rpm for 3 hours. The precursor then went through a CVD step with CH_3CN for 2 hours at 900° C. The treated material was then acid washed with 1 M HCl

for 1 hour at 60° C and rinsed with 1L of DI water. The dried material is denoted as CN_x and was recovered and stored for testing.

A final material that was synthesized for comparative testing is metal-free CN_x ($MFCN_x$), done through a referenced CVD procedure [14]. This is synthesized by generating a precursor of GO and Urea through WI. The dried precursor is then ball milled at 200 rpm for 3 hours. This material is then subjected to an ammonia (NH_3) shock treatment at 950° C for 1 hour. The final material denoted $MFCN_x$ is recovered and stored for testing.

Additional catalysts have been synthesized and tested before the writing of this paper, and their syntheses have been excluded for clarification between catalysts synthesized and tested for this paper and data used just for comparative analyzation. These include Pt-based materials and catalysts synthesized involving ammonia borane (NH_3BH_3).

ORR Testing

Testing was done in a standard three-electrode system containing a working electrode, a reference hydrogen electrode, and a platinum-coil counter electrode [13]. A catalyst ink was prepared prior to application to the working electrode tip. The ink recipe used was modified to be 5 mg of catalyst sample, 175 μL ethanol, and 48 μL of Nafion. The mixture is then sonicated in an ice bath until the catalyst is well-dispersed in the fluid. 9 μL of ink is pipetted onto the glassy carbon disk on the tip of the working electrode, resulting in a loading density of 800 $\mu g*cm^{-2}$

[13]. Stabilization cyclic voltammograms were performed on all catalysts prior to collecting data from slow CVs. The fast stabilization CVs were performed by scanning from 1.2 V to 0 V to 1.2 V at a rate of 50 $mV*s^{-1}$. Once the stabilization scans showed consistent results, the slow CVs were performed at a rate of 10 $mV*s^{-1}$ at working electrode rotation speeds of 1000 and 1600 rpm. Perchloric acid ($HClO_4$) was used as the electrolytic medium in the half-cell setup.

The resulting slow CVs can be compared according to heteroatom dopant, synthesis method, and heteroatom source material. These acquired data can then also be compared to previously tested Pt catalysts and other carbon-based catalysts to identify activity trends, after matching working electrode rotation speeds to provide accurate comparisons.

Results

Synthesis Challenges

While performing the heat treatment under inert atmosphere of a CB_y-TA catalyst, some of the GO layered over the B_2O_3 was lost to the quartz tube due to gas flow because of GO's low density. On the next synthesis of a CB_y-TA catalyst, the total mass of reactant and gas flow rate were both reduced to prevent material loss, which lead to an increased catalyst recovery rate.

While performing the first NaOH wash of a CB_y-TA sample, the solid NaOH crystals did not fully dissolve in the solution over the course of the wash, potentially due to not heating the solution or not stirring rigorously enough. However, on the second wash, the NaOH solution was vigorously stirred until all the crystals dissolved before adding the catalyst to the solution.

While performing the CVD of a CN_x catalyst, uneven and excessive catalyst growth was observed. This was addressed by reducing the CH_3CN carrier gas flow rate to lower the amount of CH_3CN through the system during the treatment.

Half-Cell Testing

Electrochemical performance metrics that are used to quantify performance are onset potential, limiting current, and half-wave potential. The onset potential is an indicator of deviance from thermodynamic equilibrium before a reaction begins to proceed. The equilibrium potential of oxygen reduction is 1.23V, but reactions are not observed until the potential generally falls below 1.00V due to kinetic limitations [8]. Pt catalysts' onset potentials have been reported over 900 mV [13], while the heteroatom-doped graphene samples generated were observed to have onsets generally around 780 mV.

The limiting current is indicative of the maximum reaction rate that can be achieved given that the mass transfer of reactants to the catalyst surface is consistent, which is true at similar working electrode rotation speeds. Therefore, it is imperative that CVs be accompanied by rotational speed as to avoid misleading results and provide an accurate description of testing conditions used for replication in future studies. In the presented CV plots, a rotation speed of 1600 rpm was used for all trials. This assures consistency in the mass flow rate of fuel to the electrode surface, and thus any variation between samples in the liming current is due to catalytic performance.

The half-wave potential is indicative of the rate at which a catalysts' reaction characteristics change from kinetically limiting to mass limiting. A half-wave potential closer to the onset potential indicates a rapid shift in reaction limitations, while a greater difference indicates that

the reaction rate on the catalyst surface changed more slowly. When comparing materials similar in onset potentials and limiting currents, the one with the higher half-wave potential is the material that more quickly approaches the limiting current at lower overpotentials, thus reflecting higher performance.

One catalyst comparison performed focused on varying the amount of dopant source material through repeated syntheses. The 10:1 B:Fe ratio had the lowest ORR performance, while lower ratios like 2:1 and 3:1 B:Fe were optimal. The boron ratio affected all electrochemical metrics, as shown by the 10:1 having a lower onset potential, limiting current, and the half-wave potential than other samples. Fine tuning ratios of boron in the finished catalysts is one way to enhance the performance of CB_y and CN_xB_y. The ratio dependent activity changes are shown by **Error! Reference source not found.**. The same principle of source optimization can be applied to nitrogen doping for both CN_x and CN_xB_y.

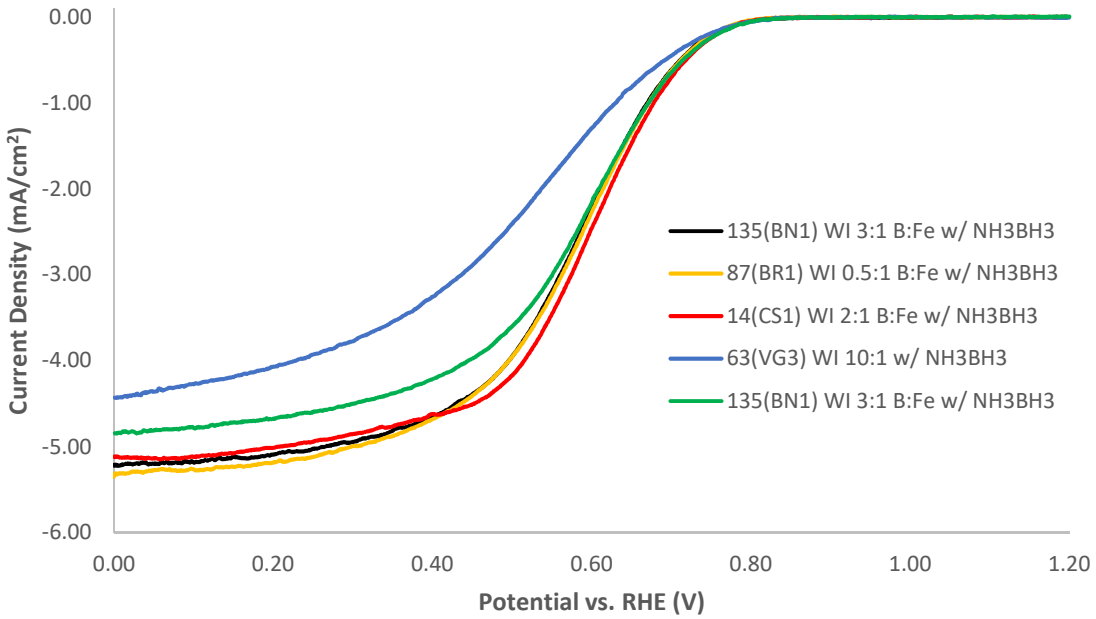

Figure 3: 1600 rpm CV results of various ratios of B:Fe in WI samples with NH_3BH_3

Another comparison shows how altering the synthesis while using the same dopant source material changes ORR performance. Here, samples were synthesized consistently using NH_3BH_3 but via three different synthesis methodologies. The WI produced the best limiting current, but the heat treatment produced the best onset potential. This data analyzation indicates that synthesis method plays a large role in the ORR activity of each final catalyst, providing another factor that can be optimized in the production of heteroatom-doped carbon-based ORR catalysts. The changes in catalytic activity due to synthesis method are shown in **Error! Reference source not found.**.

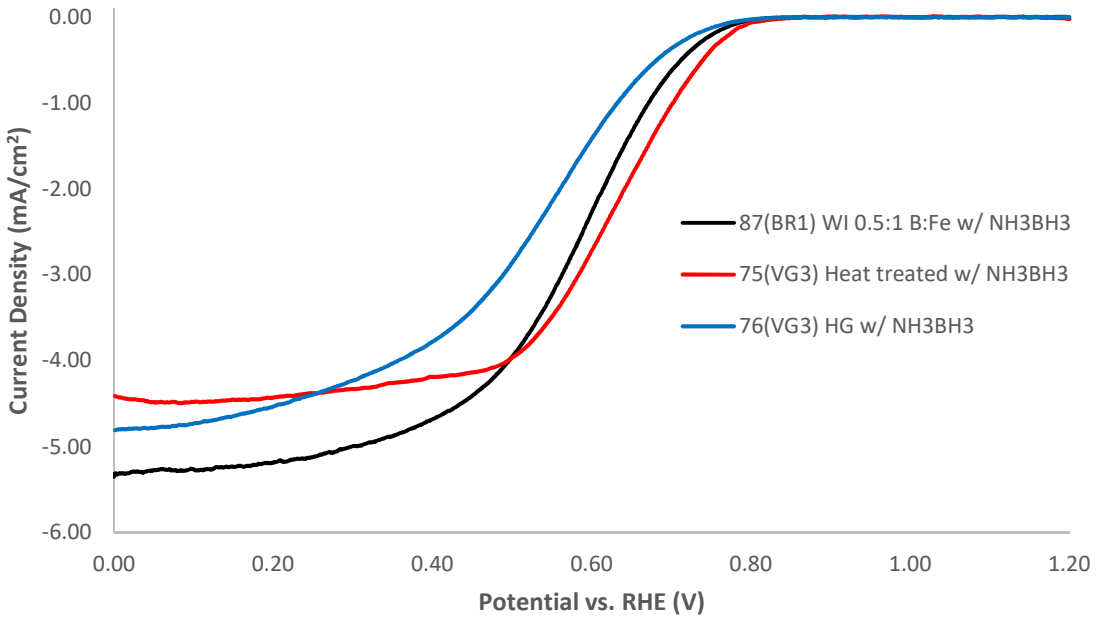

Figure 4: 1600 rpm CV results demonstrating various synthesis methods

Additionally, the data gathered demonstrates ORR performance changed based on the heteroatom dopant. Both 71(VG3), which is a CN_x sample, and 78(VG3), a CB_y sample, were outperformed in all electrochemical metrics by 14(CS1), a CN_xB_y sample. This could indicate that any mono-doped material could have better performance characteristics if it included other heteroatoms. This could be reflective of synergetic electronegative properties between boron and nitrogen resulting in increased ORR performance [8]. The variation in activity due to dopants present in the materials are shown in **Error! Reference source not found.**.

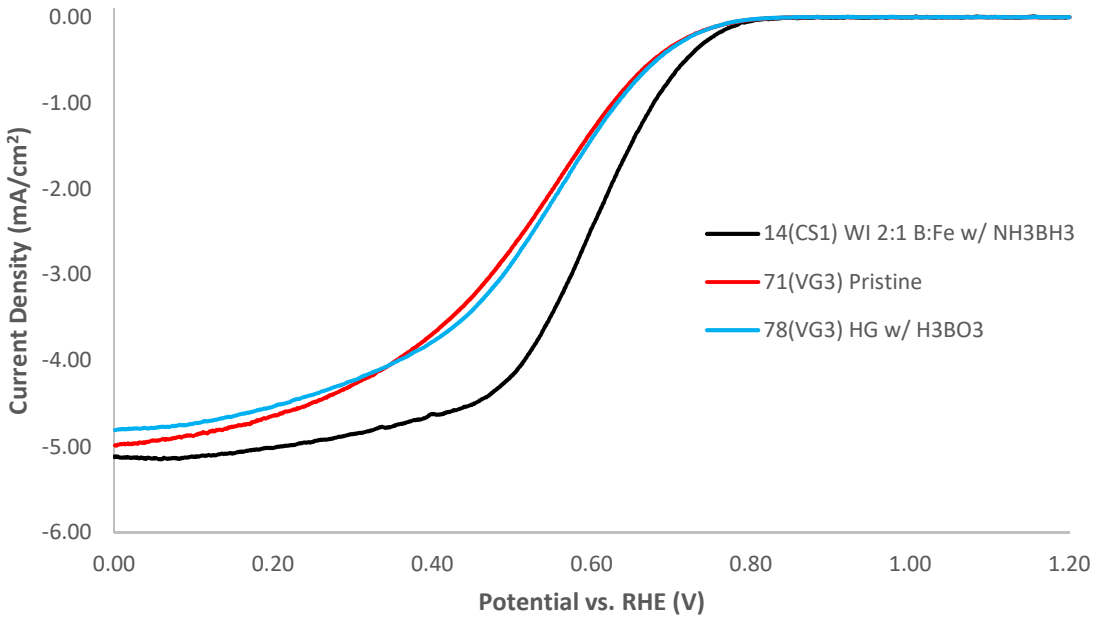

Figure 5: 1600 rpm CV results directly comparing mono- and co-doped ORR performance

According to all three electrochemical metrics recorded, various CN_xB_y samples performed best, further indicating that co-doped materials outperform their mono-doped counterparts. To restate, this is likely due to synergetic properties that emerge because of the differing electronegative properties of boron and nitrogen in the catalyst. **Error! Reference source not found.** presents all recorded electrochemical metrics, with the three best and three worst performing samples indicated by color. All previous trends discussed can be observed in the data, including co-doped samples generally outperforming mono-doped samples and the underwhelming performance of the 10:1 B:Fe WI sample compared to the other B:Fe WI samples.

Table 1: Electrochemical ORR characteristics of various catalyst samples

Sample	Type	Onset Potential (V vs RHE)	Limiting Current Density (V vs RHE)	Half-wave potential (V vs RHE)
135(BN1) WI 3:1 B:Fe w/ NH_3BH_3	CN_xB_y	0.775	-5.091	0.584
87(BR1) WI 0.5:1 B:Fe w/ NH_3BH_3	CN_xB_y	0.774	-5.183	0.584
14(CS1) WI 2:1 B:Fe w/ NH_3BH_3	CN_xB_y	0.780	-5.013	0.597
6(VG3) FeAc/MgO	CN_x	0.776	-5.097	0.600
63(VG3) WI 10:1 w/ NH_3BH_3	CN_xB_y	0.776	-4.070	0.533
71(VG3) Pristine	CN_x	0.760	-4.636	0.528
75(VG3) HT w/ NH_3BH_3	CN_xB_y	0.791	-4.426	0.629
76(VG3) HG w/ NH_3BH_3	CN_xB_y	0.772	-4.612	0.552
78(VG3) HG w/ H_3BO_3	CB_y	0.759	-4.532	0.545
135(BN1) WI 3:1 B:Fe w/ NH_3BH_3	CN_xB_y	0.781	-4.675	0.589

Conclusion

Carbon-based ORR catalysts can be modified via boron- and nitrogen-doping to approach catalytic activities for practical use. Trends indicate that co-doping with nitrogen and boron produce the most active catalysts, likely due to synergetic effects between the electronegative properties of nitrogen and boron. While carbon materials still need improvement before being a practical replacement for Pt catalysts in commercial HFCs just yet, the successful modification in ORR activity is indicative that further improvements to ORR activity can be made following additional study and experimentation.

Future work

Carbon-based ORR catalyst studied can be theoretically or experimentally continued. The work done for this study can be further optimized in attempts to generate more active boron- and nitrogen-doped materials. This includes shifting the methodology and the materials used as carbon bases and as suppliers of the heteroatoms. Additionally, the materials that were generated could be structurally analyzed through various methods such as X-ray photoelectron spectroscopy (XPS) , X-ray diffraction (XRD), or Raman spectroscopy to correlate how surface modification and specific structure can affect ORR selectivity.

Additional applications

Besides vehicular applications to replace fossil fuel systems, HFCs are promising alternatives for stationary energy sources and small portable energy sources, like batteries [15]. Some of the most promising features of HFCs are that, unlike internal combustion engines (ICEs), they are not subject to Carnot Cycle restrictions, meaning that their efficiency can reach up to 85% when effective heat capture is utilized, much better than the roughly 25% efficiency of modern ICEs [15]. Additionally, unlike batteries which have a set amount of power they can provide per full charge, HFCs can continuously generate power given an unhindered supply of fuel and air [15]. One final promising detail of growing HFC usage is that it can capture the renewability of all other types of green energy as well. HFCs effectively solve the problem of energy storage in green methods when electricity is not being produced. While solar, air, and water methods are generating electricity, some of that electricity can be used to generate hydrogen fuel for HFC systems, thus making HFCs an effective solution to energy storage problems currently faced by modern green energy solutions [15]. No matter the scale or complexity of the HFC system for mobile or stationary application, they all include precious metal-based cathodes that could benefit greatly from the development of cost effective, selective, and efficient carbon-based replacements.

Summary

Boron and nitrogen heteroatoms were successfully doped onto the surface of carbon-based materials referencing various methods and electrochemically tested for their modification to

ORR performance. Test results showed that CN_x, CB_y, and CN_xB_y all contributed to enhancing the ORR activity graphene, showing promise that heteroatom-doped graphene modification can be continued to approach that of Pt-based ORR catalysts in the future.

Bibliography

[1] "Sources of Greenhouse Gas Emissions," *United States Environmental Protection Agency*, 2019. [Online]. Available: https://www.epa.gov/ghgemissions/sources-greenhouse-gas-emissions. [Accessed: 25-Oct-2019].

[2] S. T. Thompson *et al.*, "Direct hydrogen fuel cell electric vehicle cost analysis: System and high-volume manufacturing description, validation, and outlook," *J. Power Sources*, vol. 399, pp. 304–313, Sep. 2018.

[3] W. He *et al.*, "A facile method prepared nitrogen and boron doped carbon nano-tube based catalysts for oxygen reduction," *Int. J. Hydrogen Energy*, vol. 42, no. 7, pp. 4123–4132, Feb. 2017.

[4] I. Katsounaros *et al.*, "Hydrogen peroxide electrochemistry on platinum: Towards understanding the oxygen reduction reaction mechanism," *Phys. Chem. Chem. Phys.*, vol. 14, no. 20, pp. 7384–7391, 2012.

[5] P. H. Matter, L. Zhang, and U. S. Ozkan, "The role of nanostructure in nitrogen-containing carbon catalysts for the oxygen reduction reaction," *J. Catal.*, vol. 239, no. 1, pp. 83–96, Apr. 2006.

[6] L. Yang *et al.*, "Boron-doped carbon nanotubes as metal-free electrocatalysts for the oxygen reduction reaction," *Angew. Chemie - Int. Ed.*, vol. 50, no. 31, pp. 7132–7135, Jul.

2011.

[7] D. von Deak, D. Singh, J. C. King, and U. S. Ozkan, “Use of carbon monoxide and cyanide to probe the active sites on nitrogen-doped carbon catalysts for oxygen reduction,” *Appl. Catal. B Environ.*, vol. 113–114, pp. 126–133, Feb. 2012.

[8] X. Chen, Q. Qiao, L. An, and D. Xia, “Why Do Boron and Nitrogen Doped α- And γ-graphyne exhibit different oxygen reduction mechanism? a first-principles study,” *J. Phys. Chem. C*, vol. 119, no. 21, pp. 11493–11498, 2015.

[9] L. Wang, Z. Sofer, P. Šimek, I. Tomandl, and M. Pumera, “Boron-doped graphene: Scalable and tunable p-type carrier concentration doping,” *J. Phys. Chem. C*, vol. 117, no. 44, pp. 23251–23257, Nov. 2013.

[10] L. Qu, Y. Liu, J. B. Baek, and L. Dai, “Nitrogen-doped graphene as efficient metal-free electrocatalyst for oxygen reduction in fuel cells,” *ACS Nano*, vol. 4, no. 3, pp. 1321–1326, Mar. 2010.

[11] G. Jo and S. Shanmugam, “Single-step synthetic approach for boron-doped carbons as a non-precious catalyst for oxygen reduction in alkaline medium,” *Electrochem. commun.*, vol. 25, no. 1, pp. 101–104, Nov. 2012.

[12] Z. H. Sheng, H. L. Gao, W. J. Bao, F. Bin Wang, and X. H. Xia, “Synthesis of boron doped graphene for oxygen reduction reaction in fuel cells,” *J. Mater. Chem.*, vol. 22, no. 2, pp. 390–395, Jan. 2012.

[13] K. Mamtani *et al.*, “Insights into oxygen reduction reaction (ORR) and oxygen evolution reaction (OER) active sites for nitrogen-doped carbon nanostructures (CNx) in acidic

media," *Appl. Catal. B Environ.*, vol. 220, pp. 88–97, Jan. 2018.

[14] D. Wei, Y. Liu, Y. Wang, H. Zhang, L. Huang, and G. Yu, "Synthesis of n-doped graphene by chemical vapor deposition and its electrical properties," *Nano Lett.*, vol. 9, no. 5, pp. 1752–1758, 2009.

[15] P. P. Edwards, V. L. Kuznetsov, W. I. F. David, and N. P. Brandon, "Hydrogen and fuel cells: Towards a sustainable energy future," *Energy Policy*, vol. 36, no. 12, pp. 4356–4362, 2008.

Appendix A: Tables

Table A.1: Electrochemical ORR characteristics of various catalyst samples

Sample	Type	Onset Potential (V vs RHE)	Limiting Current Density (V vs RHE)	Half-wave potential (V vs RHE)
135(BN1) WI 3:1 B:Fe w/ NH_3BH_3	CN_xB_y	0.775	-5.091	0.584
87(BR1) WI 0.5:1 B:Fe w/ NH_3BH_3	CN_xB_y	0.774	-5.183	0.584
14(CS1) WI 2:1 B:Fe w/ NH_3BH_3	CN_xB_y	0.780	-5.013	0.597
6(VG3) FeAc/MgO	CN_x	0.776	-5.097	0.600
63(VG3) WI 10:1 w/ NH_3BH_3	CN_xB_y	0.776	-4.070	0.533
71(VG3) Pristine	CN_x	0.760	-4.636	0.528
75(VG3) HT w/ NH_3BH_3	CN_xB_y	0.791	-4.426	0.629
76(VG3) HG w/ NH_3BH_3	CN_xB_y	0.772	-4.612	0.552
78(VG3) HG w/ H_3BO_3	CB_y	0.759	-4.532	0.545
135(BN1) WI 3:1 B:Fe w/ NH_3BH_3	CN_xB_y	0.781	-4.675	0.589

Appendix B: Figures

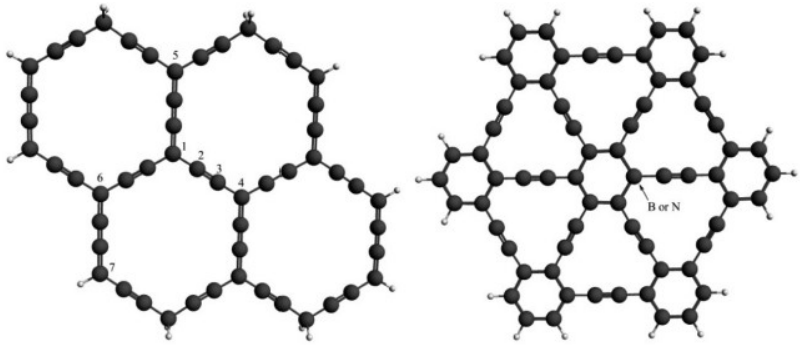

Figure B.1: Configurations of (a) α- and (b) γ-graphene w/ gray C and white H atoms [8]

$$O_2 + H^+ + e^- \rightarrow *OOH \quad (1)$$

$$*OOH + H^+ + e^- \rightarrow *O{-}H_2O \quad (2)$$

$$*O{-}H_2O + H^+ + e^- \rightarrow *OH + H_2O \quad (3)$$

$$*OH + H^+ + e^- \rightarrow H_2O \quad (4)$$

$$\text{overall:} \quad O_2 + 4H^+ + 4e^- \rightarrow 2H_2O \quad (5)$$

Figure B.2: Simulated ORR reaction mechanism [8]

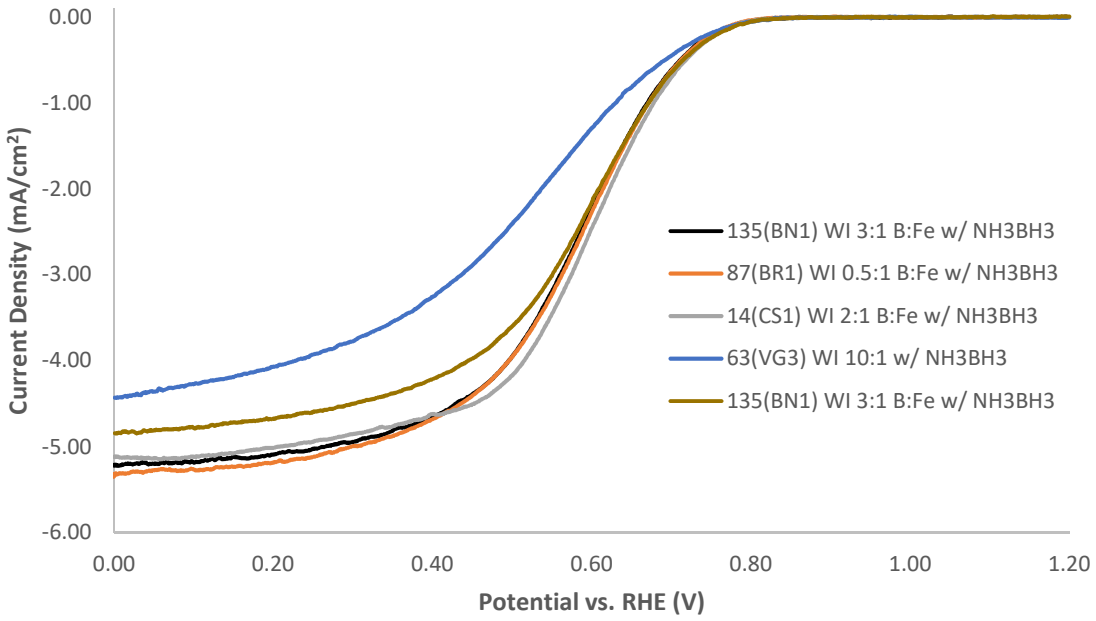

Figure B.3: 1600 rpm CV results of various ratios of B:Fe in WI samples with NH_3BH_3

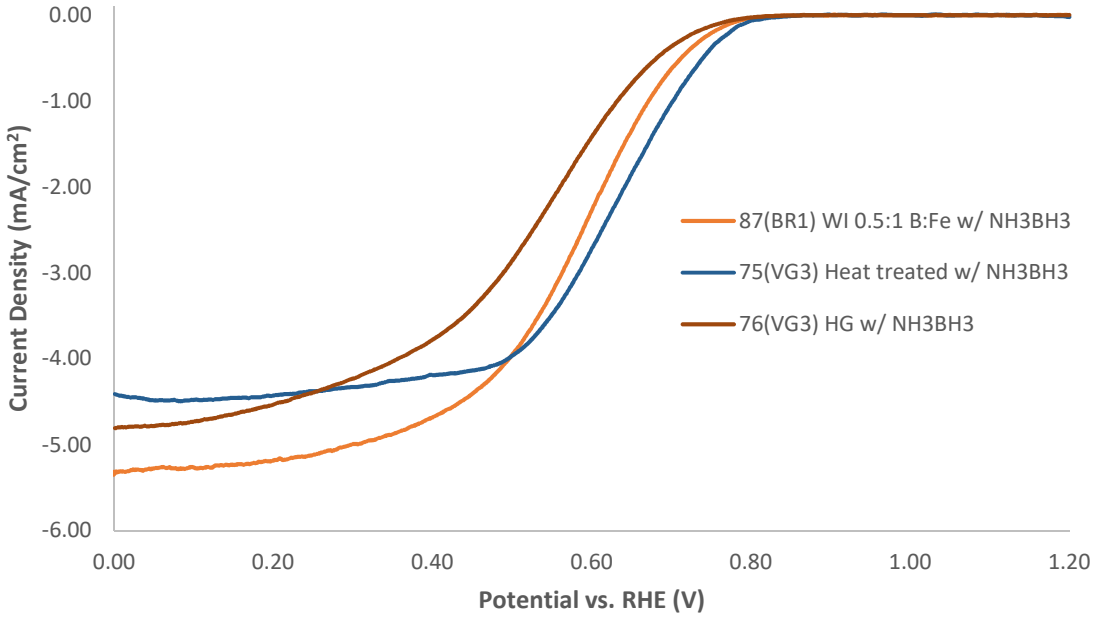

Figure B.4: 1600 rpm CV results demonstrating various synthesis methods

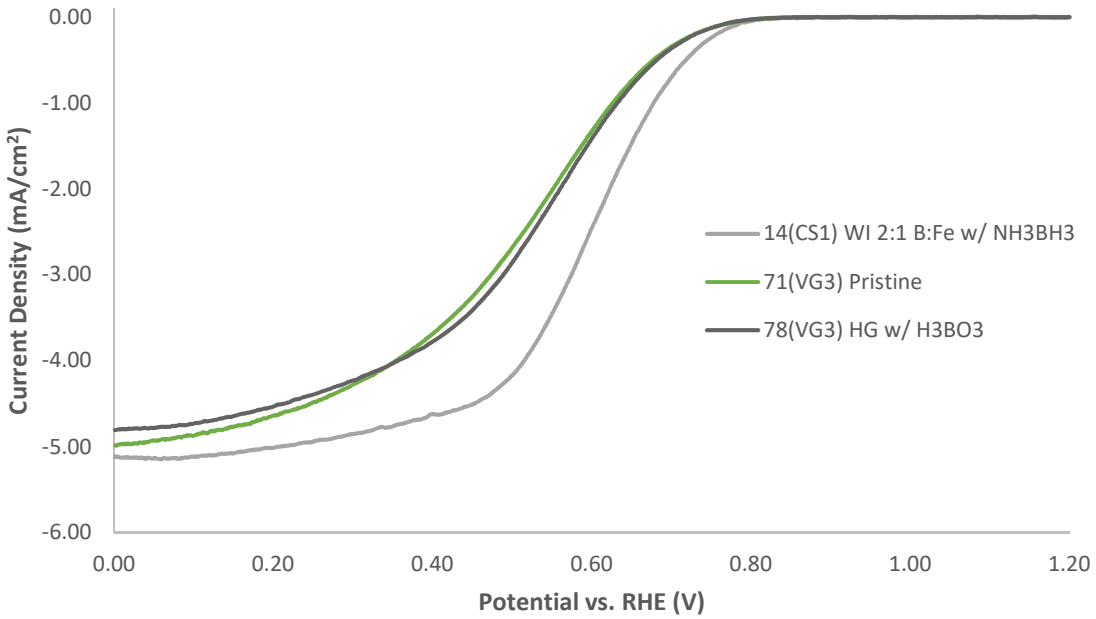

Figure B.5: 1600 rpm CV results directly comparing mono- and co-doped ORR performance